processes

MDPI

Article

Biodegradable Composite Film of Brewers' Spent Grain and Poly(Vinyl Alcohol)

Lilian Lin †, Sarah Mirkin †,‡ and Heon E. Park *

Department of Chemical and Process Engineering, University of Canterbury, Christchurch 8041, New Zealand; lilian.lin@pg.canterbury.ac.nz (L.L.); sarahmirkin1@gmail.com (S.M.)

* Correspondence: heon.park@canterbury.ac.nz; Tel.: +64-3-369-0962

† These authors contributed equally to this work.

‡ Current address: Aurecon, Christchurch 8013, New Zealand.

Abstract: Plastic pollution and food waste are two pressing global challenges that require immediate attention and innovative solutions. In this study, we address these challenges by upcycling brewers' spent grain (BSG) into biodegradable composite films. BSG, a by-product of the beer brewing process, is commonly discarded in landfills or used as animal feed. By utilizing BSG as a raw material for biodegradable films, we simultaneously reduce waste and decrease plastic pollution. To create the composite films, we employed poly(vinyl alcohol) (PVA) and glycerol as binder materials, along with hexamethoxymethylmelamine (HMMM) as a water-repelling agent. By varying the ratios of these components, we investigated the effects on film properties. Our characterization included assessing moisture uptake and tensile properties. The results revealed that the practical BSG content in the films was 20–60 wt%. Films with this composition exhibited a balance between moisture absorption and mechanical strength. The addition of glycerol improved the flexibility and toughness of the films, while HMMM reduced moisture absorption, enhancing their water resistance. This study contributes to the development of sustainable materials by showcasing the potential of upcycling BSG into valuable biodegradable films. By transforming food waste into useful applications, we reduce environmental burdens and promote a circular economy. Further research is warranted to explore the potential applications and optimize the properties of BSG-based composites.

Keywords: brewers' spent grain; mulch film; poly(vinyl alcohol); biodegradable composite film; mechanical properties; waste upcycling; food waste; glycerol; hexamethoxymethylmelamine (HMMM); moisture uptake; universal test machine; tensile tests

Citation: Lin, L.; Mirkin, S.; Park, H.E. Biodegradable Composite Film of Brewers' Spent Grain and Poly(Vinyl Alcohol). *Processes* **2023**, *11*, 2400. https://doi.org/10.3390/pr11082400

Academic Editor: Maria Angela A. Meireles

Received: 20 July 2023
Revised: 6 August 2023
Accepted: 8 August 2023
Published: 9 August 2023

1. Introduction

The usage of plastic in today's society is unsustainable, and if the current production rate continues, it is estimated that approximately 12 billion metric tons of plastic waste will be generated by 2050 [1,2]. Plastics, being highly diverse pollutants, exhibit variations in size, shape, and properties. The primary concern regarding plastic pollution lies in its longevity, as it takes hundreds of years for plastic to fully decompose into inert gases. The prolonged existence of plastics significantly impacts various ecosystems. This pressing global issue demands immediate attention and collective efforts to mitigate its extensive consequences. Even in geographically remote regions like New Zealand [3], the presence of microplastics has been detected, highlighting the pervasive nature of this problem. Containers and packaging components account for 16% of global plastic waste [2,4]. Plastic pollution negatively affects soil by altering its natural composition, microbial activity, water retention capacity, and density. In response to the ecological imperative to reduce synthetic plastic consumption and waste, there has been a significant increase in research on the properties and production of biodegradable films and membranes [5,6].

On the other hand, another issue that deserves attention is food waste. One example is brewers' spent grain (BSG) [7], which accounts for approximately 85% of the by-products

generated during the beer brewing process [8]. Globally, an estimated 35 million tons of BSG is produced each year, with 20 kg of BSG (wet basis) resulting from the production of 100 L of beer. The brewing process involves milling the barley malt, followed by mashing with water to create wort through enzymatic hydrolysis of the malt [6]. The insoluble parts of the grain settle and the wort is filtered, resulting in BSG waste. The BSG is collected while the wort continues to be processed into beer by adding hops and later yeast for fermentation and maturation [8]. BSG typically contains 70–80% moisture and is prone to spoilage due to its high protein and polysaccharide content [7], which makes it an ideal nutrient source for microbes. The high moisture content also makes transporting BSG expensive due to its excessive weight. Barley is the most used grain in breweries, comprising the germ, endosperm, seed coat, pericarp layers, and husk. BSG primarily consists of the seed coat, pericarp, and husk layers left behind after brewing. Its composition includes fiber (22–52% w/w dry basis), protein (14–31% w/w), and lignin (11–28% w/w) [8]. The majority of BSG is either sent to landfills or used as animal feed, typically sold at a cost of NZD 10 per ton of wet BSG [7]. Due to the high transportation costs and short shelf-life, BSG is primarily supplied to local dairy farmers or discarded, composted, or fermented. This presents a clear opportunity [9–12] to acquire and utilize BSG at a low cost for the production of biodegradable products. Upcycling food waste [13,14] (BSG in this study) in such products not only reduces waste but also decreases the dependence on long-lasting plastics. However, there is limited research on composite films incorporating BSG. One example is a multi-ring can-holder [15]. However, there was only 9.5% BSG in the patent application. Although the inventors claim that this can-holder is edible and environmentally benign, their oil-repelling chemical, perfluoroalkyl ethyl phosphate, falls under the category of "perfluoroalkyl and polyfluoroalkyl substances" (PFAS), which have' toxicological effects [16,17].

In our study, we aimed to develop biodegradable films that incorporate a substantial fraction of BSG and environmentally benign components to avoid similar concerns and issues. However, it should be noted that BSG alone does not possess adhesive properties to form a dimensionally stable structure of a final product. Therefore, relying solely on BSG as the main component may not result in the desired stability of the composite film. To overcome the challenge of forming a strong structure using unmodified BSG while minimizing environmental impact, we incorporated biodegradable plastic as a binder material. For this purpose, we selected poly(vinyl alcohol) (PVA) resin [18,19] as a binder. PVA was chosen due to its affordability, non-toxicity, biodegradability [20], and relatively low processing temperatures. PVA is produced through the hydrolysis of poly(vinyl acetate) in the presence of a catalyst, such as sodium hydroxide [21]. The resulting PVA can exhibit different degrees of hydrolysis (DoH), with partially hydrolyzed PVA containing 10–15 mol% acetate groups and fully hydrolyzed PVA containing 1–2 mol% acetate groups. PVA is utilized in various applications, depending on its molecular weight, DoH, and combination with other components, including fibers [22], fiber-reinforced composites [23,24], and, particularly, films [25–29]. PVA has a higher melting temperature due to the strong hydrogen bonds formed between its hydroxyl groups [30], making it suitable for shaping processes based on solution casting after dissolving in water. Polymer melt processes typically require operating temperatures above the melting point of the polymer, such as 160 °C for PLA [31]. However, it is important to note that BSG may undergo undesirable effects, such as cooking or burning, at such high temperatures. Therefore, a maximum processing temperature of 100 °C in solution casting with water is a suitable choice for incorporating BSG into composite films. This temperature allows for the effective dispersion of BSG within the film matrix while minimizing the risk of thermal degradation or other detrimental effects on the BSG particles. Hence, we employed the solution casting method to fabricate films.

In addition to PVA, we introduced two more components to our composite films. Since PVA films have a tendency to absorb moisture due to their hydrophilicity, we employed hexamethoxymethylmelamine (HMMM) [32], an FDA-approved crosslinking agent used in food packaging products [30] as a crosslinking agent, to enhance water resistance.

Crosslinking is a common method [26] to improve the water-resistance of PVA films. Another component was glycerol, which acted as a plasticizer. Plasticizers are substances that enhance the elasticity, toughness, flexibility, and stretchiness of films [33]. Considering that flexibility or stretchability of polymeric products has an important role in their functions [34], it is important to control those by choosing a proper plasticizer in the right amount. For hydrophilic polymers like PVA, plasticizers are highly effective in reducing the rigidity of the polymers. They do not chemically bind with the polymer but facilitate increased movement of polymer chains, thereby reducing intermolecular forces. This addition improves the physical properties and versatility of the film but also increases its vapor permeability. PVA is inherently rigid due to its high crystallinity and hydrogen bonding. However, for film applications, flexibility is desired, and therefore a plasticizer is commonly added. While urea is another common choice for a bioplastic plasticizer, it poses environmental concerns due to high nitrogen levels and solubility, potentially contaminating groundwater and rivers through leaching [35]. On the other hand, glycerol has been studied as a method to reduce perchlorate contamination in groundwater and has shown benefits in reducing nitrate levels through the kinetics of biological reduction by soil microorganisms [36]. As a result, we have chosen glycerol [37,38] as a plasticizer over urea. By combining BSG, PVA, glycerol, and HMMM in different proportions, we fabricated biodegradable composite films. We fabricated two sets of composite films. In the first set, while keeping the ratio of contents among PVA, glycerol, and HMMM fixed, we varied the content of BSG as an independent variable to isolate the effects of BSG. In the other set, while keeping the ratio of contents among BSG, PVA, and HMMM fixed, we varied the content of glycerol as an independent variable to isolate the effects of glycerol.

Various characterizations were performed to determine the optimal content of each component and to achieve the desired properties such as moisture uptake, film appearance, film thickness, and mechanical properties (tensile strength, ultimate strain, Young's modulus, and toughness) as dependent variables. We could determine the effects of the contents of BSG and glycerol on those properties, and eventually, those formulations can be used to fabricate PVA/BSG films for given applications.

2. Materials

Poly(vinyl alcohol) (PVA) with 88 mol% DoH was obtained from Sigma Aldrich (Burlington, MA, USA) and used as the binder material for the composite films. The molecular weights of the PVA were determined using the method described in the subsequent section, yielding $M_n = 205$ kg/mol, $M_w = 217$ kg/mol, $M_z = 235$ kg/mol, and $M_w/M_n = 1.06$, where M_n, M_w, and M_z are the number-average, weight-average, and Z-average molecular weights, respectively. M_w/M_n is the polydispersity index (PDI). Glycerol, sourced from LabServ Pronalys (analytical reagent grade, ThermoFisher, Auckland, New Zealand), served as the plasticizer in the films. Hexamethoxymethylmelamine (Cymel 303LF, Allnex, Frankfurt, Germany) was utilized as the crosslinking agent to enhance the water resistance of the composite films [30]. The brewers' spent grain (BSG) used in the study was provided by a local beer brewing company, The Fermentist (Christchurch, New Zealand).

3. Methods

3.1. Molecular Weights of PVA

Molecular weights of PVA were attained using gel permeation chromatography (GPC), GPCMax VE-2001 (Malvern, UK) with triple detectors, TDA 305 (Malvern Viscotek, Malvern, UK) at 35 °C. The three detectors include light scattering, refractive index, and viscometer. Deionized water with 2.5 mg/L of sodium azide was used as the eluent in the GPC. The addition of sodium azide into deionized water was to prevent bacterial cell growth within the GPC system. Calibration of the GPC system was carried out using a narrow-disperse poly(ethylene oxide) standard with M_w = 46,000 g/mol and PDI of 1.07 (Polymers Standard Service, Mainz, Germany). To confirm that the calibration was

performed correctly, a dextran reference with M_w = 262,000 g/mol and PDI of 1.56 (Sigma Aldrich, USA) was used to confirm the calibration by comparing the attained M_n, M_w, and M_z from GPC to their actual values. PVA was analyzed by dissolving approximately 1 mg/mL of PVA into deionized water containing 2.5 mg/L of sodium azide and implemented in the GPC for a duration of 2 h. The molecular weights attained from the GPC: M_n, M_w, and M_z.

3.2. BSG Particles Preparation

Figure 1 illustrates the preparation processes for particles and dopes and film casting. Wet BSG was obtained from a local brewery and subjected to a washing process using deionized (DI) water. The washed BSG was then dried using a VirTis General Purpose Freeze Dryer 24DX48 (SP Scientific, Pennsylvania, PA, USA) until the moisture level dropped below 14 wt%. The moisture content was determined using a moisture analyzer MA35 (Sartorius, Göttingen, Germany) at 20 °C. Subsequently, the dried BSG was milled using an Ultra Centrifugal Mill ZM 100 (Retch, Haan, Germany) with a mesh size of 75 µm. Only milled BSG particles with a size below 75 µm were utilized in the film-casting process. The resulting particle size distribution was determined as follows. A photo image of the BSG particles was captured using a stereoscopic microscope (Olympus SZX10, Tokyo, Japan). The obtained image was analyzed using ImageJ software. The area of each particle in the image was measured, and the particle diameter was calculated under the assumption that each particle resembled a disk in the image. Throughout the remainder of this paper, the term "BSG" refers to dried and milled BSG particles with a diameter of 75 µm or lower.

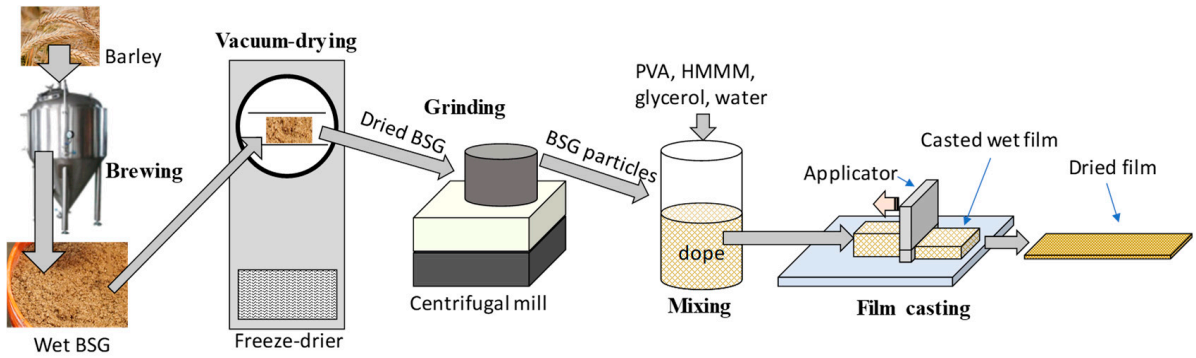

Figure 1. Preparation processes for particles and dopes and film casting (not to scale).

3.3. Film Casting and Thickness Measurement

Calendaring [39] is not suitable for hydrophilic polymers like PVA due to the close proximity of the melting and thermal degradation points caused by the strong hydrogen bonds within the polymer chains [40]. Therefore, we employed the solution casting method to fabricate our films (Figure 1), which involved dissolving PVA and other components in a liquid and mixing them with the BSG particle dispersion within the polymer matrix. To prepare the PVA/water solution, PVA pellets were dissolved in deionized (DI) water at 90 °C and thoroughly mixed using a magnetic stirrer to create a 10 wt% solution. Glycerol was then added to the solution, and the liquid was stirred at 80 °C for 10 min. BSG, HMMM, and water were added to the solution to achieve a fraction of water of 0.9. The mixture was further homogenized using a planetary mixer AR100 (Thinky, Tokyo, Japan) at 2200 rpm for 5 min, and the visual uniformity of the mixture was confirmed. The suspension was stirred at 70 °C on a stirring hot plate for 45 min [33] to induce crosslinking. The compositions of the dope for film casting are provided in Table 1 for a basis of a total of 1 g of dope. We fixed the ratio among PVA, glycerol, and HMMM in a set of composites (B1 through B6) to isolate the effects of BSG. The BSG content gradually increases from 0 (B1) to 90 wt% (B6) while maintaining a constant ratio of PVA:glycerol:HMMM = 3.4:1.8:1.0. The glycerol content in polymeric films range from 20 to 40% [41], and we chose a midpoint of 29% of glycerol content for B1. We performed a series of experiments to determine the ratio between PVA

and HMMM to minimize moisture absorption, and we found that the content of HMMM should be at least 30% of PVA content to have a significant effect on HMMM (the data are not shown in this report.) We kept the above ratios for the other composites of B2 through B6.

Table 1. Compositions of the dope of 1 g for film casting. The numbers in the table will be in % after drying, except water.

Code	BSG (mg)	PVA (mg)	Glycerol (mg)	HMMM (mg)	DI Water (mL)	Ratio
B1	0.0	54.8	29.0	16.1	0.9	PVA:glycerol:HMMM = 3.4:1.8:1.0
B2	20.0	43.9	23.2	12.9	0.9	
B3	40.0	32.9	17.4	9.7	0.9	
B4	60.0	21.9	11.6	6.5	0.9	
B5	80.0	11.0	5.8	3.2	0.9	
B6	90.0	5.5	2.9	1.6	0.9	
G1	43.8	43.8	0.0	12.5	0.9	BSG:PVA:HMMM = 3.5:3.5:1.0
G2	42.4	42.4	3.0	12.1	0.9	
G3	41.1	41.1	6.0	11.8	0.9	
G4	39.4	39.4	10.0	11.3	0.9	

On the other hand, in another set of composites (G1 through G4), we fixed the ratio among BSG, PVA, and HMMM to isolate the effects of glycerol. The glycerol content increases from 0 (G1) to 10 wt% (G4) while maintaining a constant ratio of BSG:PVA:HMMM = 3.5:3.5:1.0. We tried to maximize the amount of BSG without lowering mechanical strength too much, so we chose a 1:1 ratio of PVA and BSG while keeping the ratio between PVA and HMMM the same as the previous composites set. After the film is dried, the values in Table 1, except for water, indicate the component content in percentage.

The prepared dope was applied onto a glass plate positioned on an optical breadboard. A coating of the dope was then achieved by using an adjustable film applicator, ensuring a consistent coating thickness of 1.5 mm at a temperature of 20 °C. The film casting setup was covered, leaving one side open, and allowed to rest at 20 °C for 24 h. Following this, the film was carefully detached from the glass plate and subjected to drying in a lyophilizer (Virtis General Purpose Freeze Dryer 35L EL, Scientific Products, Gardiner, NY, USA) for 24 h. Subsequently, the films were stored in a vacuum oven (OV11, Jeiotech, Daejeon, Republic of Korea) at 20 °C until they were ready for further characterizations.

The local thicknesses of the casted films were determined using a digital indicator (ID-C112CMXB, Mitutoyo, Sakado, Japan). The tip of the indicator touched the surface, which had been facing the air during the casting process of the film, to measure thicknesses. The minimum thickness was measured at three locations that were visually thin or flat, while the maximum thickness was measured at three locations that were visually thicker than the thin parts.

3.4. Tensile Tests

To assess the mechanical properties of the films, tensile tests were conducted using a universal testing machine (model 5965, Instron, Norwood, MA, USA). The tests aimed to obtain parameters such as tensile strength (σ_{TS}), ultimate tensile strain, Young's modulus (E_T), and toughness. The dimensions of the samples used for testing were as follows: length of 10 cm and width of 1 cm. The testing procedure followed the guidelines outlined in ASTM D638-22 Standard Test Method for Tensile Properties of Plastics [42]. The tests were performed at a crosshead speed of 50 mm/s and a temperature of 20 °C. Tensile stress (σ_T) was calculated using the formula:

$$\sigma_T = \frac{F_T}{wd} \quad (1)$$

where F_T is the tensile force, w is the width of the strip, and d is the minimum thickness of the strip. The tensile strength (σ_{TS}) is the maximum tensile stress was attained using:

$$\sigma_{TS} = \frac{F_{T,max}}{wd} \quad (2)$$

where $F_{T,max}$ is the maximum tensile force applied. The tensile strain (ε_T) was obtained by:

$$\varepsilon_T = \frac{\Delta L}{L_0} \quad (3)$$

where ΔL is the tensile displacement, L_0 is the initial length of the strip, and the ultimate (tensile) strain, ε_{UT} is the maximum tensile strain when the sample breaks. The Young's (elastic) modulus (E_T) was determined as the slope of the σ_T versus ε_T plot with its linear regime:

$$E_T = \frac{\Delta \sigma_T}{\Delta \varepsilon_T} \quad (4)$$

The toughness of the material was assessed by calculating the total area under the curve of the σ_T versus ε_T plot.

3.5. Hydrophilicity and Moisture Uptake

The hydrophilicity of the film product was evaluated by measuring the moisture uptake. The film was placed in a humidified tub at 100% relative humidity (RH) and 20 °C for 15 min. Subsequently, the wet film was patted-dry and re-weighed. The hydrophilicity of the composite films was quantified using two methods as follows:

$$\mathrm{MU_{dry}}(\%) = \frac{m - m_0}{m_0} \times 100\ (\%) \quad (5)$$

$$\mathrm{MU_{wet}}(\%) = \frac{m - m_0}{m} \times 100\ (\%) \quad (6)$$

where m is the mass of the wet film, and m_0 is the mass of the dried film. Equation (5) shows how much moisture a dried film can uptake, while Equation (6) shows the moisture content in a film.

3.6. Statistical Analysis

Three sample repeats were used for each type of test. The obtained data were subjected to statistical analysis using Analysis of Variance (ANOVA), which employs *F*-tests to evaluate the effect of variances in the characteristics of the samples [43]. Additionally, Student's *t*-test was employed. A significance level of $p < 0.05$ was considered statistically significant. Both were performed using Microsoft Excel 2019.

4. Results and Discussion

4.1. Particle Size Distribution of Milled BSG Particles

The particle size distribution of the dried and milled BSG particles is presented in Figure 2. As anticipated, the distribution confirms that the particle diameter is smaller than the mill size (75 μm). The majority of the particles exhibit smaller sizes due to the milling process, which operates with a sieve-like mechanism. Within the milling chamber, rotating pins facilitate the grinding of the grain, allowing particles to pass through the sieve when they reach a small enough size. It is worth noting that no particles smaller than 15 μm were observed in the distribution.

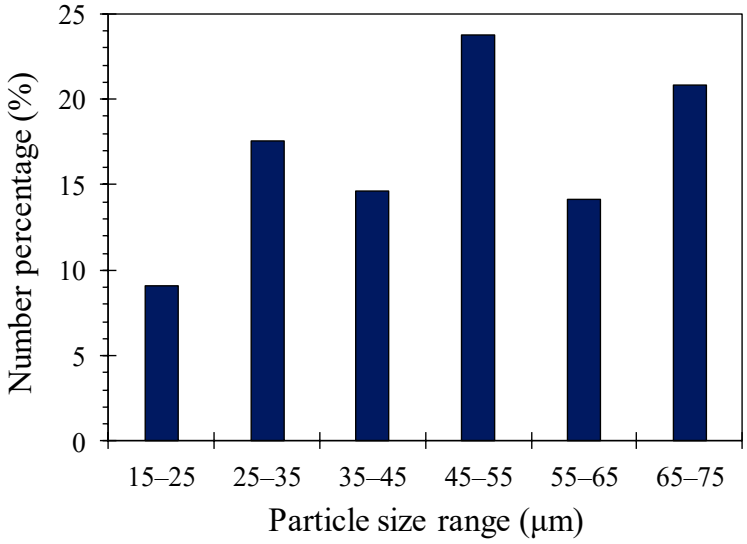

Figure 2. Particle size (diameter) distribution of the dried and milled BSG.

4.2. Moisture Uptake

Figure 3 illustrates the impact of BSG content on the moisture uptake of the composite films (B1 through B6) after exposure to 100% RH for 15 min. Figure 3a represents the moisture uptake calculated using Equation (5), which indicates how much moisture a dried film can absorb. On the other hand, Figure 3b displays the moisture uptake determined by Equation (6), which signifies the moisture content in the wet film. The results indicate that the BSG content in the films does not have a significant effect on the moisture uptake by films. Both MU_{dry} = 150% and MU_{wet} = 60% are relatively high. These findings differ from a study conducted by Chiellini et al. [30], which investigated PVA and apple pomace. Their results showed MU_{wet} ranging from 16% to 22% after exposure to 95% RH for 28 days. The higher moisture uptake observed in our study may be attributed to the presence of glycerol as a plasticizer in our films. Among the composite films, B1 has no BSG but the highest amount of PVA (55%) and HMMM (16.1%). Consequently, one might anticipate reduced water-absorbing materials and increased water resistance. Notably, B1 also contains the highest glycerol content of 29%. Since the solubility of water in glycerol is higher than that in PVA, the increased glycerol content contributes to the overall moisture uptake capability. Chiellini et al. [30] also reported no significant difference in moisture uptake between PVA and apple pomace. Considering the similarity in composition between BSG and apple pomace, it can be inferred that the moisture uptake between BSG and PVA would exhibit minimal variation. Consequently, the higher solubility of water in glycerol compared to BSG further supports the balanced moisture uptake observed in the samples from B1 to B6. The competition between the reduced moisture-absorbing materials and increased water resistance in B1, along with the elevated glycerol content, leads to a comparable moisture uptake capability among samples B1 through B6.

To isolate the effect of glycerol content, we maintained a constant ratio among BSG, PVA, and HMMM while varying only the glycerol content for samples G1 through G4. Figure 4 depicts the impact of glycerol content on the moisture uptake of the composite films after exposure to 100% RH for 15 min. Figure 4a represents the moisture uptake calculated using Equation (5), indicating how much moisture a dried film can absorb. Figure 4b displays the moisture uptake determined by Equation (6), representing the moisture content in the wet film. The results clearly demonstrate that moisture uptake, or hydrophilicity, increases with the glycerol content, as indicated by MU_{dry} = 110–215% or MU_{wet} = 52–68%. This trend can be attributed to the high affinity of glycerol for water, facilitated by its three hydroxyl groups that form hydrogen bonds with water molecules. Importantly, considering that the total amount of PVA, BSG, and HMMM decreases as the glycerol content increases from G1 to G4, the observed trend in Figure 4 can be primarily

attributed to the impact of glycerol itself. The strong interaction between glycerol and water further supports the increased moisture uptake observed in the films.

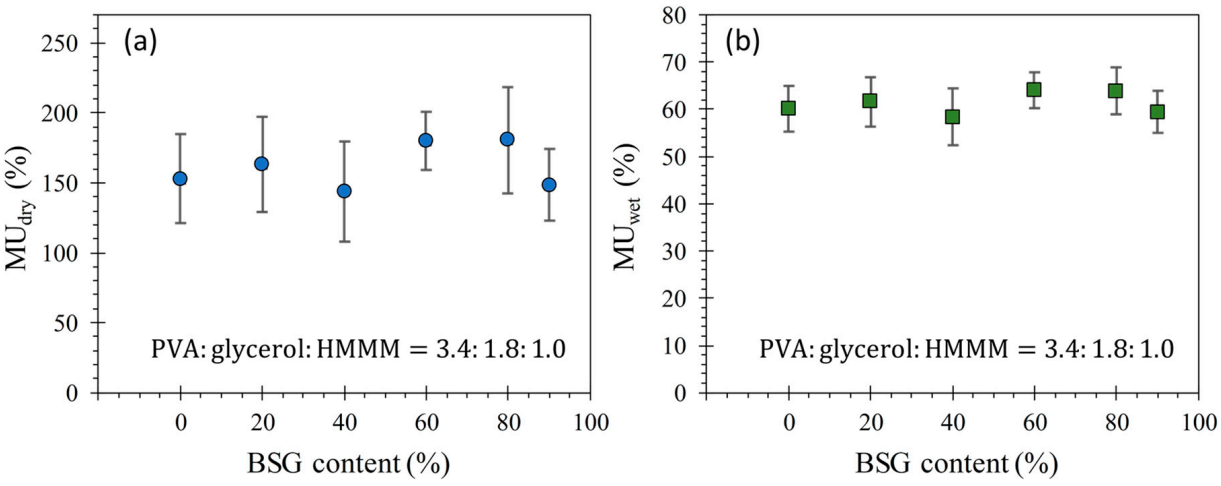

Figure 3. Effect of BSG content on the moisture uptake of composite films of B1 through B6. (**a**) Moisture uptake relative to the mass of dried film; (**b**) Moisture uptake relative to the mass of wet film. The mass ratio among components other than BSG is shown on the plot. The error bars are the standard deviations.

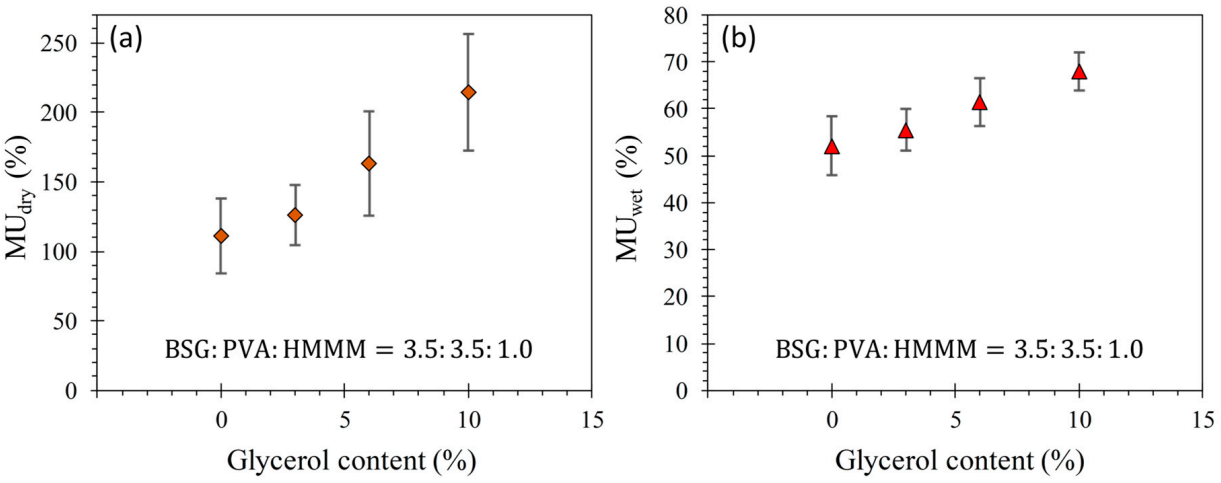

Figure 4. Effect of glycerol content on the moisture uptake of composite films of G1 through G4. (**a**) Moisture uptake relative to the mass of dried film; (**b**) Moisture uptake relative to the mass of wet film. The mass ratio among components other than glycerol is shown on the plot. The error bars are the standard deviations.

In addition to increasing the overall moisture uptake of the film, the addition of glycerol as a plasticizer to PVA has the effect of reducing the film's crystallinity [44]. This reduction in crystallinity is attributed to the introduction of defects in the lattice structure caused by the highly polar and hydrophilic nature of glycerol, which allows for easier movement of the polymer chains [45]. The decreased crystallinity of the PVA component in the film further contributes to its moisture uptake [46]. Thus, the glycerol content plays a crucial role in balancing the flexibility, moisture uptake, and mechanical properties (discussed in Section 4.4) of BSG/PVA films and should be carefully considered during film design. Overall, the films produced in this study exhibit a clear ability to absorb moisture. This characteristic makes them suitable for applications where high moisture absorption is desired or not a concern. One potential application is a disposable laundry bag that can be submerged directly in water along with laundry. In this case, both the PVA and glycerol

components of the film will dissolve in warm or hot water, which is desired. Considering that BSG has a more rigid nature compared to PVA (discussed in Section 4.4), it can serve as a scrubbing element. Subsequently, all the components comprising the laundry bag can be easily washed away. Moisture uptake is related to biodegradation, but its kinetics study is out of the scope of this study, so we have not performed quantitative biodegradation studies, which can be one of the future directions of studying PVA/BSG films to broaden its applications as a biodegradable composite.

4.3. Film Morphology and Thickness

Figure 5 provides a visual representation of the appearance of the composite films after casting. The inclusion of BSG in the composite films has a noticeable impact on both their appearance and texture. The film without any BSG content (B1) appears slightly turbid and exhibits elasticity. Films with lower BSG content (20% and 40%, B2 and B3) are opaque with a light brown color and display slight brittleness. As the BSG content increases to 60 and 80% (B4 and B5), the films become highly opaque and stiff. B6 with 90% BSG could not maintain its dimension due to high brittleness. Additionally, these films (B4 through B6) show a less homogeneous appearance, with small clumps that become apparent as the films dry, resulting in an uneven surface. The uneven surface and clumping of BSG particles in the dope are likely responsible for these observations. When the BSG content is high, the BSG particles can stack on top of each other, leading to the formation of multiple layers. In contrast, when the BSG content is low, the particles tend to form a single layer within the film. There is no significant difference observed among G1 through G4 in terms of the glycerol content (ranging from 0 to 10%), as the BSG content remains relatively constant (ranging from 39.4 to 43.8%). However, an increase in glycerol content resulted in a significant increase in the flexibility of the composite films. The addition of glycerol as a plasticizer allowed for increased mobility and reduced intermolecular forces within the film, leading to enhanced flexibility and improved mechanical properties.

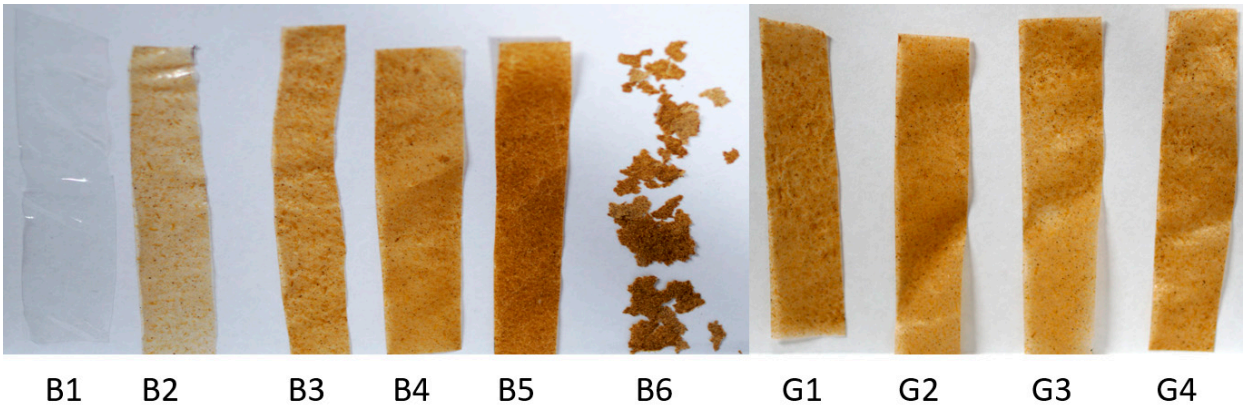

Figure 5. Appearance of roughly cut, solution-casted films.

Figure 6a illustrates the local thickness distribution observed in the composite films as the BSG content increases. The maximum particle size (diameter) of BSG particles used was 0.075 mm, the gap in the film casting applicator (representing the initial thickness of the dope layer) was 1.5 mm, and the water content was 90%, and, thus, a simple estimation of the thickness of a dried film would be 0.15 mm. However, the minimum local thickness was smaller than that value. The minimum local thickness likely indicates areas in the film where the BSG content is minimal, representing predominantly the thickness of the binder components (PVA, glycerol, and HMMM). It is expected that both the minimum and maximum local thicknesses of the film increase with increasing BSG content. The sudden jump in thickness observed at 60% BSG (B4) can be attributed to the clumping of BSG particles, suggesting that the dopes were not uniformly compounded and did not form a homogeneous mixture. This finding aligns with the observations made by Chiellini

et al. [30] that dopes with fiber content exceeding 50% are not practical for producing useful films due to inhomogeneous thickness. The difference between the maximum and minimum local thicknesses of the films reflects the uniformity of the film, with a smaller difference indicating a more uniform film. As the BSG content increases, the uniformity of the film decreases, likely due to the clumping of BSG particles within the dope. The large difference between the minimum and maximum thicknesses of the films is not ideal for a film product as it indicates non-uniformity, resulting in varying physical properties throughout the film. Therefore, achieving a homogeneous mixture of components is crucial for the successful development of this type of composite film.

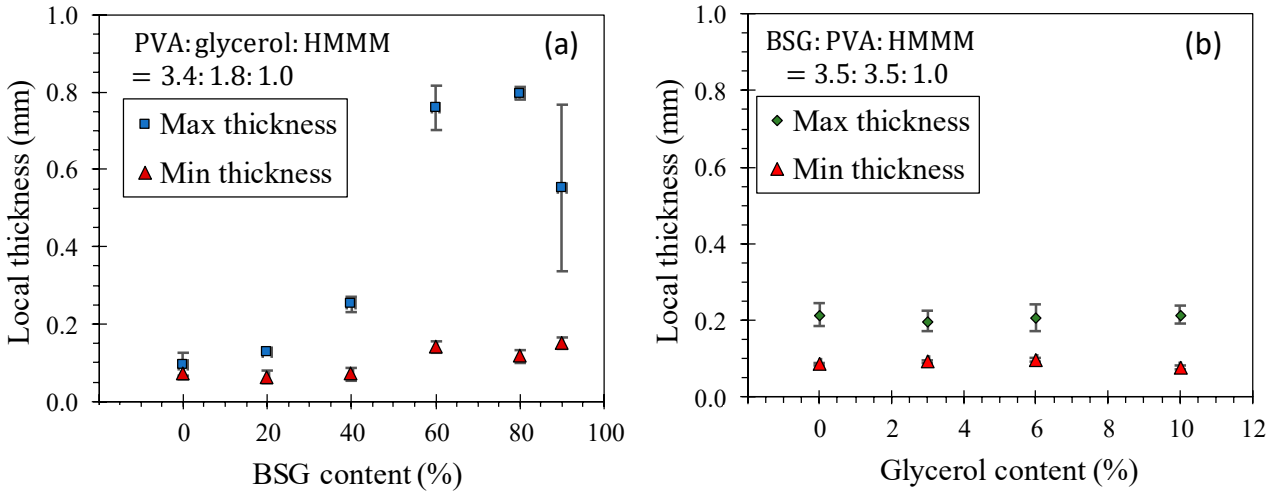

Figure 6. Maximum and minimum local film thicknesses. (**a**) Effect of BSG content for B1 through B6; (**b**) Effect of glycerol content for G1 through G4. The error bars are the standard deviations.

In contrast, Figure 6b demonstrates that the glycerol content has no significant effect on the thickness distribution, unlike the BSG content. Statistically, the difference between the maximum and minimum thicknesses remains independent of the glycerol content ranging from 0% to 10%. This can be attributed to the relatively small variation in BSG content (ranging from 43.8% to 39.4%), considering the significant effect of BSG content on the thickness variations (Figure 6a). This finding provides more evidence that the thickness homogeneity of the film primarily relies on the BSG content.

4.4. Mechanical Properties

Figure 7 illustrates the impact of BSG content on the tensile properties of the composite films (B1 through B5). Tensile tests for B6 were not possible due to natural ruptures of the film, as observed in Figure 5. Both tensile strength and ultimate strain demonstrate a decreasing trend with increasing BSG content (Figure 7a). The tensile strength remains relatively constant up to 40% BSG (32.9% PVA, 17.4% glycerol, and 9.7% HMMM) and then exhibits a significant drop at 60% BSG (21.9% PVA, 11.6% glycerol, and 6.5% HMMM). This decrease can be attributed to the highly brittle nature of films with higher BSG content. A similar trend was observed for a composite of PVA/cottonseed shell [29]. As the BSG content increases, the added amounts of PVA, HMMM, and glycerol decrease. The reduction in the amount of binding materials (PVA and HMMM) contributes to the decrease in tensile strength. Conversely, the reduction in the amount of plasticizer (glycerol) can increase the tensile strength. Up to 40% BSG, such counteracting combination results in a relatively similar tensile strength. However, from 60% BSG onward, the effect of the reduced amount of binding materials becomes dominant, leading to a significant drop in tensile strength.

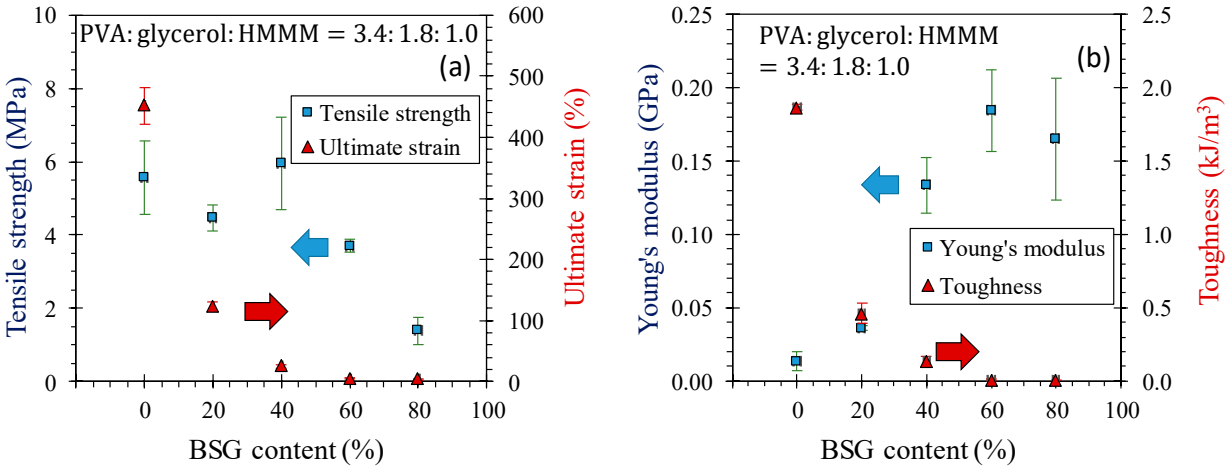

Figure 7. Effects of BSG content on the tensile properties of B1 through B5. (**a**) On tensile strength and ultimate strain; (**b**) On Young's modulus and toughness. The error bars are the standard deviations. The blue and red arrows indicate the axes on which the data are plotted.

In terms of ultimate strain, a significant decrease is observed from 20% BSG (43.9% PVA, 23.2% glycerol, and 12.9% HMMM), indicating that the film becomes more brittle as the BSG content increases. With increasing BSG content, the film loses its ability to stretch, resulting in a decrease in ultimate strain. This significant decrease in ultimate strain occurs at a lower BSG content compared to the decrease in tensile strength. This is because the proportions of binding materials and glycerol are all decreasing with increasing BSG content, resulting in a reduction in elasticity in the films. In the case of fibrous fillers [47], it is common to observe an increase in both tensile strength and ultimate strain with increasing filler content. However, the unique structure of BSG and the occurrence of adhesive (interfacial) failure between BSG particles and the binder and/or the cohesive failure in the binder led to the opposite trends in this study. As a result, the addition of BSG resulted in a decrease in both tensile strength and ultimate strain of the composite films. These trends align with the findings of other studies on PVA/apple pomace composites [30]. However, since their data show a dramatic drop in ultimate strain with 10% apple pomace and a continuous drop in tensile strength from 10% apple pomace, the data from this study suggest that there is more flexibility in adjusting the BSG content within the composite films.

In Figure 7b, it is observed that the Young's modulus of the composite films significantly increases with BSG content up to 40% BSG, indicating that BSG imparts greater rigidity compared to the other components. Films with 60% and 80% BSG do not show a significant difference in Young's modulus, suggesting that the rigidity is primarily governed by the BSG content and reaches a saturation point at 60% BSG. This increase in Young's modulus differs from previous studies on PVA/apple pomace composites [30], which reported a continuous decrease in Young's modulus with increasing filler content. Furthermore, Figure 7b demonstrates that the toughness of the films dramatically decreases at lower BSG content and generally follows the trend of ultimate strain. Therefore, it can be expected that films with 60% or higher BSG content will not exhibit high toughness. The optimal BSG content for the composite films should depend on the specific application. However, based on the results, a range of 20% to 60% BSG content is recommended to balance the desired properties for the intended application.

Figure 8a shows the effect of glycerol content on the tensile properties of the composite films (G1 to G4). Up to a glycerol content of 3%, there is no significant impact on the tensile strength. However, beyond this content, the tensile strength decreases significantly while the ultimate strain increases. This suggests that glycerol acts as a plasticizer, exerting its plasticizing effect on the films. To observe the full plasticization effect, a glycerol content of more than 3% is required in applications. These trends align with previous studies on PVA/apple pomace composites, which also reported similar effects of glycerol content up

to 50% [30]. It is worth noting that we aimed to limit the addition of glycerol to maintain BSG as the main component in the composite films. In this study, it is evident that the plasticizing effect of glycerol increases the mobility of the PVA chains, thereby reducing the stress required for deformation. Consequently, the films become easier to stretch and exhibit decreased rigidity. This phenomenon is clearly observed in Figure 8b, where the Young's modulus (a measure of rigidity) continuously decreases with increasing glycerol content, resulting in greater flexibility of the films. As a result, the toughness of the films increases with glycerol content. The relationship between toughness and glycerol content aligns with the relationship observed between ultimate strain and glycerol content, as previously shown in Figure 7.

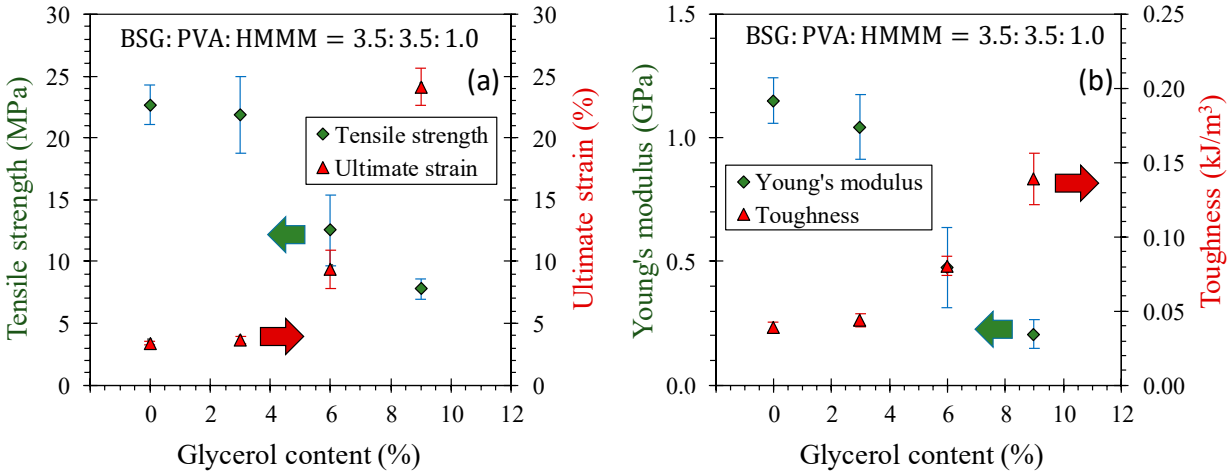

Figure 8. Effects of glycerol content on the tensile properties of G1 through G4. (**a**) On tensile strength and ultimate strain; (**b**) On Young's modulus and toughness. The error bars are the standard deviations. The green and red arrows indicate the axes on which the data are plotted.

5. Conclusions

This study successfully developed biodegradable composite films using brewers' spent grain (BSG) as a filler material, poly(vinyl alcohol) (PVA) as a binder, and hexamethoxymethylmelamine (HMMM) as a water-repelling agent. The practical BSG content ranged between 20% and 60%, providing a balance between film properties such as uniformity in thickness, water absorption, and mechanical strengths. The films exhibited significant moisture uptake, making them suitable for applications where water absorption is desirable, such as in laundry bags. The addition of HMMM can help reduce moisture absorption. This is beneficial for applications where excessive moisture absorption could lead to functional issues during storage. However, further research is required to enhance the water repellence of the films for applications requiring dry conditions. The mechanical properties of the films were influenced by the BSG content, with a decrease in tensile strength and ultimate strain observed as the BSG content increased. The addition of glycerol improved the flexibility and toughness of the films, making them more resistant to brittleness. In summary, this study highlights the potential of utilizing BSG as a sustainable resource in the development of biodegradable composite films. The findings contribute to the growing body of research on eco-friendly alternatives to traditional plastics and provide insights for the design and optimization of BSG-based films for various applications.

Author Contributions: Conceptualization, S.M. and H.E.P.; methodology, S.M., L.L. and H.E.P.; software, S.M. and L.L.; validation, S.M., L.L. and H.E.P.; formal analysis, S.M. and L.L.; investigation, S.M. and L.L.; resources, H.E.P.; data curation, S.M. and L.L.; writing—original draft preparation, L.L. and H.E.P.; writing—review and editing, L.L., S.M. and H.E.P.; visualization, L.L. and S.M.; supervision, H.E.P.; project administration, H.E.P.; funding acquisition, H.E.P. All authors have read and agreed to the published version of the manuscript.

Funding: This research was funded by the Department of Chemical and Process Engineering at the University of Canterbury, New Zealand.

Data Availability Statement: The data presented in this study are available on request from the corresponding author.

Acknowledgments: The authors thank Kirsten Taylor at The Fermentist, New Zealand, for supplying BSG and sharing ideas, Scott Auger at Allnex for providing HMMM, and Matthew Cowan, Rayleen Fredericks, Michael Sandridge, Stephen Beuzenberg, Glenn Wilson, and Garrick Thorn in the Department of Chemical and Process Engineering at the University of Canterbury, New Zealand for their support. S.M. thanks Ken Morison in the same department for the use of the Ultra Centrifugal Mill.

Conflicts of Interest: The authors declare no conflict of interest.

References

1. Windsor, F.M.; Durance, I.; Horton, A.A.; Thompson, R.C.; Tyler, C.R.; Ormerod, S.J. A catchment-scale perspective of plastic pollution. *Glob. Chang. Biol.* **2019**, *25*, 1207–1221. [CrossRef]
2. Geyer, R.; Jambeck, J.R.; Law, K.L. Production, use, and fate of all plastics ever made. *Sci. Adv.* **2017**, *3*, e1700782. [CrossRef]
3. Mazlan, N.; Lin, L.; Park, H. Microplastics in the New Zealand Environment. *Processes* **2022**, *10*, 265. [CrossRef]
4. Ahmed, S. (Ed.) *Bio-Based Materials for Food Packaging: Green and Sustainable Advanced Packaging Materials*; Springer: Berlin/Heidelberg, Germany, 2018.
5. Maria, T.M.C.; de Carvalho, R.A.; Sobral, P.J.A.; Habitante, A.M.B.Q.; Solorza-Feria, J. The effect of the degree of hydrolysis of the PVA and the plasticizer concentration on the color, opacity, and thermal and mechanical properties of films based on PVA and gelatin blends. *J. Food Eng.* **2008**, *87*, 191–199. [CrossRef]
6. Hussain, Z.; Ullah, S.; Yan, J.; Wang, Z.; Ullah, I.; Ahmad, Z.; Zhang, Y.; Cao, Y.; Wang, L.; Mansoorianfar, M.; et al. Electrospun tannin-rich nanofibrous solid-state membrane for wastewater environmental monitoring and remediation. *Chemosphere* **2022**, *307*, 135810. [CrossRef]
7. Fărcaş, A.; Tofană, M.; Socaci, S.; Mudura, E.; Scrob, S.; Salanţă, L.; Mureşan, V. Brewers' spent grain—A new potential ingredient for functional foods. *J. Agroaliment. Process. Technol.* **2014**, *20*, 137–141.
8. Lynch, K.M.; Steffen, E.J.; Arendt, E.K. Brewers' spent grain: A review with an emphasis on food and health. *J. Inst. Brew.* **2016**, *122*, 553–568. [CrossRef]
9. Emmanuel, J.K.; Nganyira, P.D.; Shao, G.N. Evaluating the potential applications of brewers' spent grain in biogas generation, food and biotechnology industry: A review. *Heliyon* **2022**, *8*, e11140. [CrossRef]
10. Jackowski, M.; Niedźwiecki, Ł.; Jagiełło, K.; Uchańska, O.; Trusek, A. Brewer's Spent Grains—Valuable Beer Industry By-Product. *Biomolecules* **2020**, *10*, 1669. [CrossRef]
11. Estévez, A.; Padrell, L.; Iñarra, B.; Orive, M.; San Martin, D. Brewery by-products (yeast and spent grain) as protein sources in rainbow trout (Oncorhynchus mykiss) feeds. *Front. Mar. Sci.* **2022**, *9*, 862020. [CrossRef]
12. Zeko-Pivač, A.; Tišma, M.; Žnidaršič-Plazl, P.; Kulisic, B.; Sakellaris, G.; Hao, J.; Planinić, M. The Potential of Brewer's Spent Grain in the Circular Bioeconomy: State of the Art and Future Perspectives. *Front. Bioeng. Biotechnol.* **2022**, *10*, 870744. [CrossRef] [PubMed]
13. Mirani, A.; Goli, M. Optimization of cupcake formulation by replacement of wheat flour with different levels of eggplant fiber using response surface methodology. *Food Sci. Technol.* **2022**, *42*, e52120. [CrossRef]
14. Thakur, A.; Sharma, S.; Ganjoo, R.; Assad, H.; Kumar, A. Anti-Corrosive Potential of the Sustainable Corrosion Inhibitors Based on Biomass Waste: A Review on Preceding and Perspective Research. *J. Phys. Conf. Ser.* **2021**, *2267*, 012079. [CrossRef]
15. Lauria, G.A.; Cendejas, J.F.; Malpica, M.A.; Joshina, J.K. Edible Multi-Ring Can-Holder and Methods for Manufacturing Edible Can-Holders. U.S. 15/590,754, 18 January 2018.
16. Buck, R.C.; Franklin, J.; Berger, U.; Conder, J.M.; Cousins, I.T.; de Voogt, P.; Jensen, A.A.; Kannan, K.; Mabury, S.A.; van Leeuwen, S.P.J. Perfluoroalkyl and polyfluoroalkyl substances in the environment: Terminology, classification, and origins. *Integr. Environ. Assess. Manag.* **2011**, *7*, 513–541. [CrossRef]
17. Brendel, S.; Fetter, É.; Staude, C.; Vierke, L.; Biegel-Engler, A. Short-chain perfluoroalkyl acids: Environmental concerns and a regulatory strategy under REACH. *Environ. Sci. Eur.* **2018**, *30*, 9. [CrossRef]
18. Finch, C.A. *Polyvinyl Alcohol—Development*; Wiley: Hoboken, NJ, USA, 1992.
19. Goodship, V.; Daniel, J. *Polyvinyl Alcohol: Materials, Processing and Applications*; Smithers Rapra: Shrewsbury, UK, 2009.
20. Ben Halima, N. Poly(vinyl alcohol): Review of its promising applications and insights into biodegradation. *RSC Adv.* **2016**, *6*, 39823–39832. [CrossRef]
21. Aruldass, S.; Mathivanan, V.; Mohamed, A.R.; Tye, C.T. Factors affecting hydrolysis of polyvinyl acetate to polyvinyl alcohol. *J. Environ. Chem. Eng.* **2019**, *7*, 103238. [CrossRef]
22. Sakurada, I. *Polyvinyl Alcohol Fibers*; Marcel Dekker: New York, NY, USA, 1985.
23. Tan, B.; Ching, Y.; Poh, S.; Abdullah, L.; Gan, S. A Review of Natural Fiber Reinforced Poly(Vinyl Alcohol) Based Composites: Application and Opportunity. *Polymers* **2015**, *7*, 2205–2222. [CrossRef]

24. Mahardika, M.; Asrofi, M.; Amelia, D.; Syafri, E.; Rangappa, S.M.; Siengchin, S. Tensile Strength and Moisture Resistance Properties of Biocomposite Films Based on Polyvinyl Alcohol (PVA) with Cellulose as Reinforcement from Durian Peel Fibers. *E3S Web Conf.* **2021**, *302*, 02001. [CrossRef]
25. Gaikwad, K.K.; Lee, J.Y.; Lee, Y.S. Development of polyvinyl alcohol and apple pomace bio-composite film with antioxidant properties for active food packaging application. *J. Food Sci. Technol.* **2015**, *53*, 1608–1619. [CrossRef]
26. Liu, B.; Zhang, J.; Guo, H. Research Progress of Polyvinyl Alcohol Water-Resistant Film Materials. *Membranes* **2022**, *12*, 347. [CrossRef] [PubMed]
27. Panda, P.K.; Sadeghi, K.; Seo, J. Recent advances in poly (vinyl alcohol)/natural polymer based films for food packaging applications: A review. *Food Packag. Shelf Life* **2022**, *33*, 100904. [CrossRef]
28. Zulkiflee, I.; Fauzi, M.B. Gelatin-Polyvinyl Alcohol Film for Tissue Engineering: A Concise Review. *Biomedicines* **2021**, *9*, 979. [CrossRef] [PubMed]
29. Tian, G.; Li, L.; Li, Y.; Wang, Q. Water-Soluble Poly(vinyl alcohol)/Biomass Waste Composites: A New Route toward Ecofriendly Materials. *ACS Omega* **2022**, *7*, 42515–42523. [CrossRef]
30. Chiellini, E.; Cinelli, P.; Imam, S.H.; Mao, L. Composite Films Based on Biorelated Agro-Industrial Waste and Poly(vinyl alcohol). Preparation and Mechanical Properties Characterization. *Biomacromolecules* **2001**, *2*, 1029–1037. [CrossRef]
31. Lin, L.; Lee, Y.; Park, H.E. Recycling and rheology of poly(lactic acid) (PLA) to make foams using supercritical fluid. *Phys. Fluids* **2021**, *33*, 067119. [CrossRef]
32. Chen, L.; Imam, S.H.; Gordon, S.H.; Greene, R.V. Starch- polyvinyl alcohol crosslinked film— performance and biodegradation. *J. Environ. Polym. Degrad.* **1997**, *5*, 111–117. [CrossRef]
33. Regubalan, B.; Pandit, P.; Maiti, S.; Nadathur, G.T.; Mallick, A. Potential Bio-Based Edible Films, Foams, and Hydrogels for Food Packaging. In *Bio-Based Materials for Food Packaging*; Springer: Singapore, 2018; pp. 105–123.
34. Liu, Y.; Zhang, Y.; An, Z.; Zhao, H.; Zhang, L.; Cao, Y.; Mansoorianfar, M.; Liu, X.; Pei, R. Slide-Ring Structure-Based Double-Network Hydrogel with Enhanced Stretchability and Toughness for 3D-Bio-Printing and Its Potential Application as Artificial Small-Diameter Blood Vessels. *ACS Appl. Bio Mater.* **2021**, *4*, 8597–8606. [CrossRef]
35. Prasad, R. Fertilizer urea, food security, health and the environment. *Curr. Sci.* **1998**, *75*, 677–683.
36. Sarria, M.; Gonzales, J.M.; Gerrity, D.; Batista, J. Biological Reduction of Nitrate and Perchlorate in Soil Microcosms: An Electron Donor Comparison of Glycerol, Emulsified Oil, and Mulch Extract. *Groundw. Monit. Remediat.* **2018**, *39*, 32–42. [CrossRef]
37. Westhoff, R.P.; Kwolek, W.F.; Otey, F.H. Starch-Polyvinyl Alcohol Films–Effect of Various Plasticizers. *Starch—Stärke* **1979**, *31*, 163–165. [CrossRef]
38. Lawton, J.W.; Fanta, G.F. Glycerol-plasticized films prepared from starch—Poly(vinyl alcohol) mixtures: Effect of poly(ethylene-co-acrylic acid). *Carbohydr. Polym.* **1994**, *23*, 275–280. [CrossRef]
39. Mitsoulis, E. Chapter 11—Calendering of polymers. In *Advances in Polymer Processing: From Macro- to Nano- Scales*; Thomas, S., Weimin, Y., Eds.; Woodhead Publishing: Athens, Greece, 2009; pp. 312–351.
40. Chen, N.; Li, L.; Wang, Q. New technology for thermal processing of poly(vinyl alcohol). *Plast. Rubber Compos.* **2013**, *36*, 283–290. [CrossRef]
41. Jantrawut, P.; Chaiwarit, T.; Jantanasakulwong, K.; Brachais, C.H.; Chambin, O. Effect of plasticizer type on tensile property and in vitro indomethacin release of thin films based on low-methoxyl pectin. *Polymers* **2017**, *9*, 289. [CrossRef]
42. *ASTM D638-22*; Standard Test Method for Tensile Properties of Plastics. ASTM International: West Conshohocken, PA, USA, 2022.
43. Rouder, J.N.; Engelhardt, C.R.; McCabe, S.; Morey, R.D. Model comparison in ANOVA. *Psychon. Bull. Rev.* **2016**, *23*, 1779–1786. [CrossRef]
44. Lv, C.; Liu, D.; Tian, H.; Xiang, A. Non-isothermal crystallization kinetics of polyvinyl alcohol plasticized with glycerol and pentaerythritol. *J. Polym. Res.* **2020**, *27*, 66. [CrossRef]
45. Porta, R.; Sabbah, M.; Di Pierro, P. Bio-Based Materials for Packaging. *Int. J. Mol. Sci.* **2022**, *23*, 3611. [CrossRef]
46. Lim, L.Y.; Wan, L.S.C. The Effect of Plasticizers on the Properties of Polyvinyl Alcohol Films. *Drug Dev. Ind. Pharm.* **2008**, *20*, 1007–1020. [CrossRef]
47. Kim, E.; Park, H.; Lopez-Barron, C.; Lee, P. Enhanced Foamability with Shrinking Microfibers in Linear Polymer. *Polymers* **2019**, *11*, 211. [CrossRef]